A new look at reflection seismic data from the Central Caledonian Transect across the Scandinavian Peninsula

Christopher Juhlin[1], Rodolphe Lescoutre[2], Bjarne Almqvist[1]

[1]Dept. of Earth Sciences, Uppsala University, Uppsala, Sweden
5 [2]Mantle8 sas, 6 rue de Chamechaude, 38360 Sassenage, France

Correspondence to: Christopher Juhlin (christopher.juhlin@geo.uu.se)

Abstract. This study revisits seismic reflection data from the central Scandinavian Caledonides, initially acquired during campaigns in the late 1980s and early 1990s. Previous analyses faced challenges in merging and imaging due to varying trace spacing and data gaps, particularly in the western parts. To address these limitations, we spatially resampled the data to
10 a consistent trace spacing, carefully merged segments, and migrated the entire merged section. This approach resulted in a revised seismic profile, with notable changes in the western section where the image reveals key differences compared to earlier interpretations. The updated profile indicates near-continuous reflections across merged segments, resolving issues of abrupt breaks present in some prior publications. Enhanced imaging in the western section unveils new structural details, including collapsed diffractions and shorter reflective segments, offset from one another. These reflecting segments in the
15 Skardöra antiform are interpreted as representing dolerite sills that were once continuous over a larger area, but have been offset by normal faulting. This reinterpretation suggests a significantly thinner Upper Allochthon in the west than in previous interpretations. These results emphasize the importance of careful data integration and migration for seismic interpretation, shedding new light on the structural complexity of the western Scandinavian Caledonides. The study contributes to refining geological models and advancing understanding of the region's tectonic history.

1 Introduction

20 A major effort to acquire reflection seismic data across the central Scandinavian Caledonides was carried out in the late 1980s and early 1990s (e.g. Hurich et al., 1989; Palm et al., 1991; Juhojuntti et al., 2001). Results from these campaigns have been presented and interpreted earlier, in the form of line drawings or seismic sections, either in part or as a continuous profile. Lescoutre et al. (2022) provides the most recent presentation of the entire merged data set, spanning a distance of over 200 km, from western Trondelag in Norway to east of the Caledonian Front in Sweden. In merging the data from the
25 different campaigns one problem that has not been properly addressed is the lack of a comprehensive migrated image in the western part of the transect. This has been hampered by differences in trace spacing between the various campaigns and not handling the overlap and gaps in an optimal manner. In this short communication we present a new version of the data set in which we have spatially resampled all data to a fixed trace spacing, merged the various campaigns more carefully and then

30   migrated the entire seismic profile at one time. This results in a somewhat different image in the western part of the profile where some important details differ from previous presentations, while the eastern part of the seismic image is essentially the same as that presented in Juhojuntti et al. (2001) and Lescoutre et al. (2022). In this paper we first review the available data, present the processing strategy and results, and finally discuss the implications for structural interpretation in the western part of the profile.

2 Geological Setting

The structural setting of the central Scandinavian Caledonides has been studied for well over a century (Törnebohm, 1888; Gee and Stephens, 2020, and references therein). These studies have contributed to major advances in understanding of fold-and-thrust belts and more specifically to the understanding on how they were formed. Closure of the Iapetus Ocean during the Silurian period, leading to a full continent-continent collision between the paleocontinents Baltica and Laurentia in the

40   early Devonian (~400 Ma), was the initial phase of their formation. During the closure stage, sediments and sedimentary rocks from the Baltica passive margin were subducted and partially returned and thrust onto Baltica. A stack of thrusted sheets developed, where some of the units were transported more than 400 km onto Baltica (Gee and Stephens, 2020). This stack of allochthons is typically divided into different units depending on their position and origin in the stack, and consist of the Uppermost, Upper, Middle and Lower allochthons, which overly the parautochtonous/autochthons Precambrian

45   basement (Table 1).

Starting at the stratigraphically uppermost unit, the Uppermost allochthon comprises rocks of Laurentian affinity. The Upper allochthon, including the Köli Nappe complex, consists of remnants of oceanic crust in the form of gabbros that have in part been serpentinized, and sedimentary rocks that were metamorphosed (i.e., phyllites). The Uppermost and Upper allochthons experienced greenschist grade metamorphism.

50   Continuing down the tectonostratigraphy, the Middle allochthon (including the Seve nappe complex), forms the central part of the stack. These rocks experienced the highest-grade metamorphic conditions in the entire stack, with widespread evidence for granulite facies conditions in the middle part of the Seve nappe complex (Arnbom, 1980), and more recent evidence for ultrahigh pressure conditions as indicated by the presence of microdiamond inclusions in garnet (Majka et al., 2014; Klonowska et al., 2017). The Lower Seve Nappe complex of the Middle allochthon mainly consists of para- and

55   orthogneisses formed at amphibolite grade conditions. Jeanneret et al. (2022) recently used Ti-in-quartz geothermobarometry to constrain the peak metamorphic conditions of the Lower Seve to upper amphibolite/lowermost eclogite facies conditions, exceeding 1 GPa pressure and 600 °C. The lowermost parts of the Middle allochthon, consisting of the Särv and Offerdal Nappes, have similar protolith as the Seve Nappe complex, but experienced significantly lower grade metamorphic conditions. The sedimentary rocks that make up the Särv Nappe originate from the passive margin of Baltica and have been

60   frequently intruded by mafic dolerites that were emplaced during the initial rifting and opening of the Iapetus Ocean ~600 Ma. Notably, metamorphosed equivalents of these dolerites exist also in the overlying Seve Nappe complexes.

The Lower allochthon consists of a succession of sedimentary rock units that range in age from the Cryogenian (>700 Ma) to Silurian (~420 Ma) periods. In the regions of the central Scandinavian Caledonides, this succession is also referred to as the Jämtlandian Nappes. During orogeny, these sedimentary units formed parts of the foreland basin, with deformation taking

65 place in the form of duplexing and local overthrusting of units within the Lower allochthon. The metamorphic grade of these units is generally greenschist facies. Tectonostratigraphically, the Alum shale makes up the lowermost part of the Lower allochthon, and marks the sole thrust or décollement of the nappe stack. Although duplexing can make for some complicated local tectonostratigraphic relationships, the Alum shale generally forms the boundary to the underlying autochtonous basement.

70

Table 1: Tectonostratigraphy, Central Scandinavian Caledonides (Norway and Sweden) based on publications by Robinson and Roberts (2008), Gee and Stephens (2020), Saalman et al. (2021) and Jakob et al. (2022).

Tectonostratigraphic level	Sub-units		
	Norway (central/southern)	*Sweden (Jämtland)*	*Original terrane*
Uppermost allochthon	Helgeland, Rödingsfjället, Fauske	Rödingsfjället	Laurentia affinity
Upper allochthon	Gula (Støren, Meråker Nappes)	Köli	Iapetus Ocean derived
Middle allochthon	Blåhø Nappe	Seve Nappe Complex	Baltica margin
	Sætra Nappe	Särv Nappe	
	Risberget Nappe	Tännäs Augen Gneiss Nappe	
Lower allochthon	Various, depending on location (Oyangen formation, Åmotsdal quartzite, Gjevilvatnet)	Jämtland Nappes	
Autochthon/para-autochthon	Baltica basement/gneiss	Precambrian granite, porphyry and gneisses	Crystalline basement

The underlying Precambrian crystalline basement underneath the allochthonous units is made up of mainly of granitoids

75 (granodiorite and quartzmonzonite) and volcanic porphyry (rhyolite, dacite, trachytes), which were recently dated by Andersson et al. (2022). The granites range in age from ~1690 to 1660 Ma, whereas the porphyries are significantly younger with ages ranging from 1670-1650 Ma (Andersson et al., 2022). A detailed transect of the Lower Allochthon and crystalline basement was recently obtained through the COSC-2 scientific drilling project (Lehnert et al., 2024; Lorenz et al., 2022). The drilled section contains well-preserved felsic porphyries, whose age ranged from ~1660 to ~1650 Ma. The whole-rock

80 chemical composition of these porphyries are identical to porphyries originating from the Transcandinavian Igneous Belt (TIB) in the nearby Fennoscandian Shield. These porphyries and related granitoids have been widely intruded by dolerite dikes related to different intrusion generations, with the most abundant in central Sweden being the Central Scandinavian Dolerite Group (CSDG; Söderlund et al., 2006). Dolerite sheets identified in the COSC-2 borehole were dated using U-Pb

baddeleyite geochronology, with two sets of preliminary ages (Lescoutre et al., 2022). The older age is ~1470 Ma, predating

85   the CSDG, whereas the second set of ages range from 1270-1260 Ma, overlapping with the CSDG. It is evident that the crystalline basement has in places been involved in Caledonian deformation, such as the tectonic window that makes up the Mullfjället antiform. Brittle deformation observed in the basement shows in part Caledonian ages, as demonstrated by K-Ar ages of fault gouges in basement just east of the present-day Caledonian foreland boundary (Almqvist et al., 2023).

3 Data

90   Figure 1 shows the general geology of the study area and the locations of the profiles included in this work. We have followed the labelling of Palm et al. (1991) for the different segments for the data acquired in 1987 and 1988. For the extensions to the east we have labelled the 1990 extension as segment I and the 1992 extension as segment J. For the segment west of Meråker, Norway (referred to as the Western Half in Roberts and Hurich (2018)), we have labelled this segment A. Digital stacked data exist further west of segment A, but have not been included in this contribution. Acquisition

95   parameters for the various segments are summarized in Table 2. As can be noted in Table 2 and in Figure 1, the greatest variability and overlap between segments can be found in the western part of the survey (segments A to F). A more detailed overview of this area is shown in Figure 2.

Table 1: Overview of seismic acquisition. For source type: E – explosive, V – vibroseis.

Segment	A	B, C	D, H	E, G	F	I	J
Approximate length (km)	45	19	15, 25	25, 18	6		
Source spacing (m)	40	200	c. 4800	400	200	50	50
Source type	V	E	E	E	E	V	V
Receiver spacing (m)	40	25	50	50	25	50	50
Channels	96	96	96	96	96	48	48
Fold	48	12	1	12	12	24	24
Record length (s)	10	20	20	20	20	10	10
Sample interval (ms)		2	2	2	2	4	4
Year acquired	1987	1987	1988	1988	1987	1990	1992

100
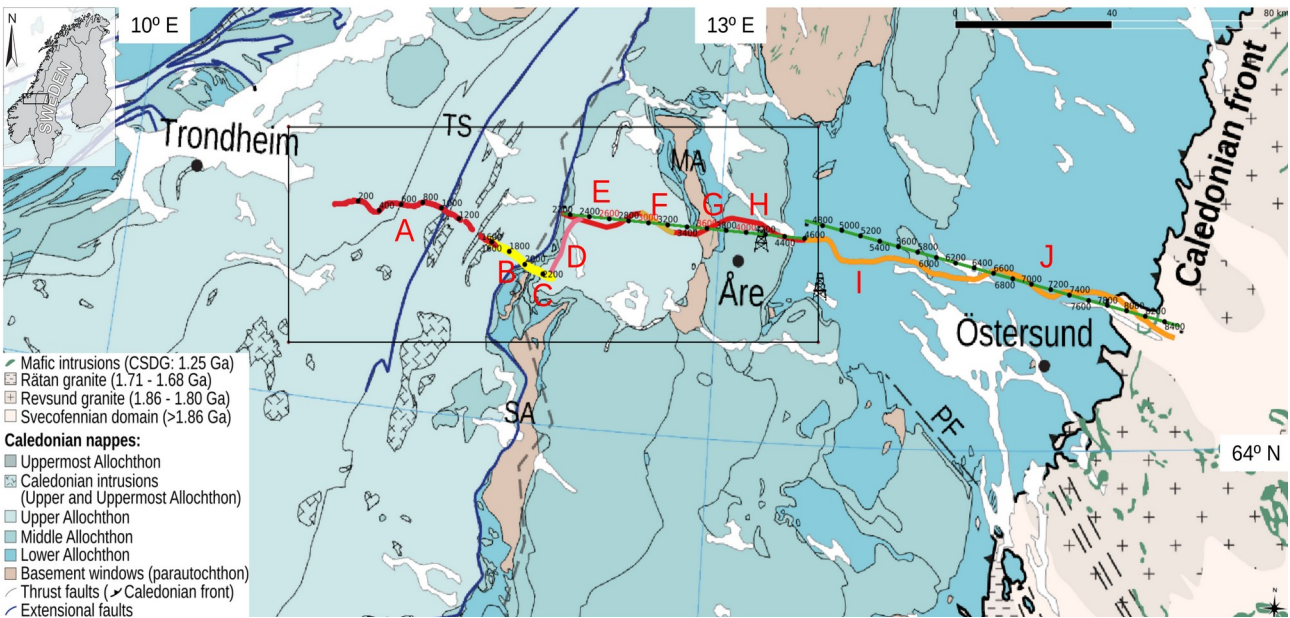
Figure 1: Location map showing the different segments discussed in this paper. The geological map is the one used by Lescoutre et al. (2022). Segments with similar acquisition parameters are coded with the same colour. Segments A, B and C were processed along crooked lines following the acquisition roads while segments E to J were projected onto two straight lines (coloured green).
105 **CDP numbers correspond to those presented on the composite stacked and migrated sections presented in this paper.**
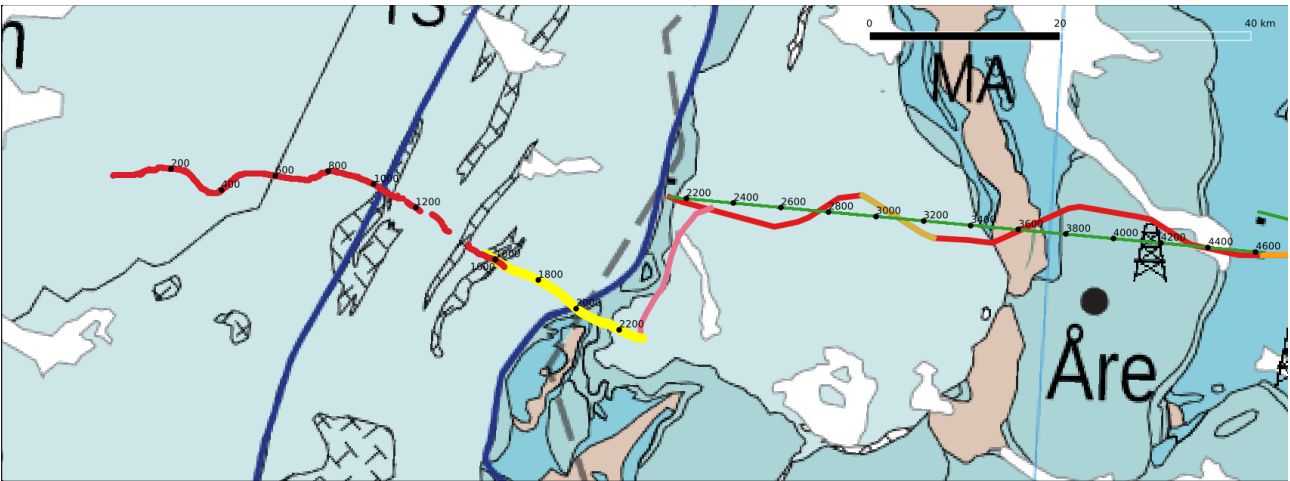

Figure 2: Detailed geometry showing the overlap of segments A and B on the Norwegian side and the connection between segment C to segment E via segment D on the Swedish side. Note that the coordinates plotted for segments A, B and C are midpoints as
110 **calculated from source and receiver coordinates in the SEGY headers. CDP coordinates were not available in the headers and may differ somewhat from the midpoints. Geological map based on Lescoutre et al. (2022).**

4 Method

It would have been advantageous to have merged the source gathers from all the segments into one data set and reprocessed the combined parts as a single profile. However, segments A, B and C were only available as stacked sections in SEGY file

115 format, while segment D was only available on paper in the report by Palm et al. (1991). Segments E to H were previously processed as a single profile and presented in Juhojuntti et al. (2001), as were segments I and J. Due to these constraints, the previously processed data have been used in this contribution, except for segment D which was digitized and reformatted to SEGY as described in Sopher (2018). Note that segments E to J are still available as raw source gathers. Given that the maximum receiver spacing is 50 m (resulting in a CDP spacing of 25 m) we have resampled segments A, B and C to a trace

120 spacing of 25 m on the stacked sections. Segments E to J were already processed with a CDP spacing of 25 m. This provides a consistent trace spacing of 25 m on all the profiles that are included in the combined stacked section which can be migrated as a single section.

6
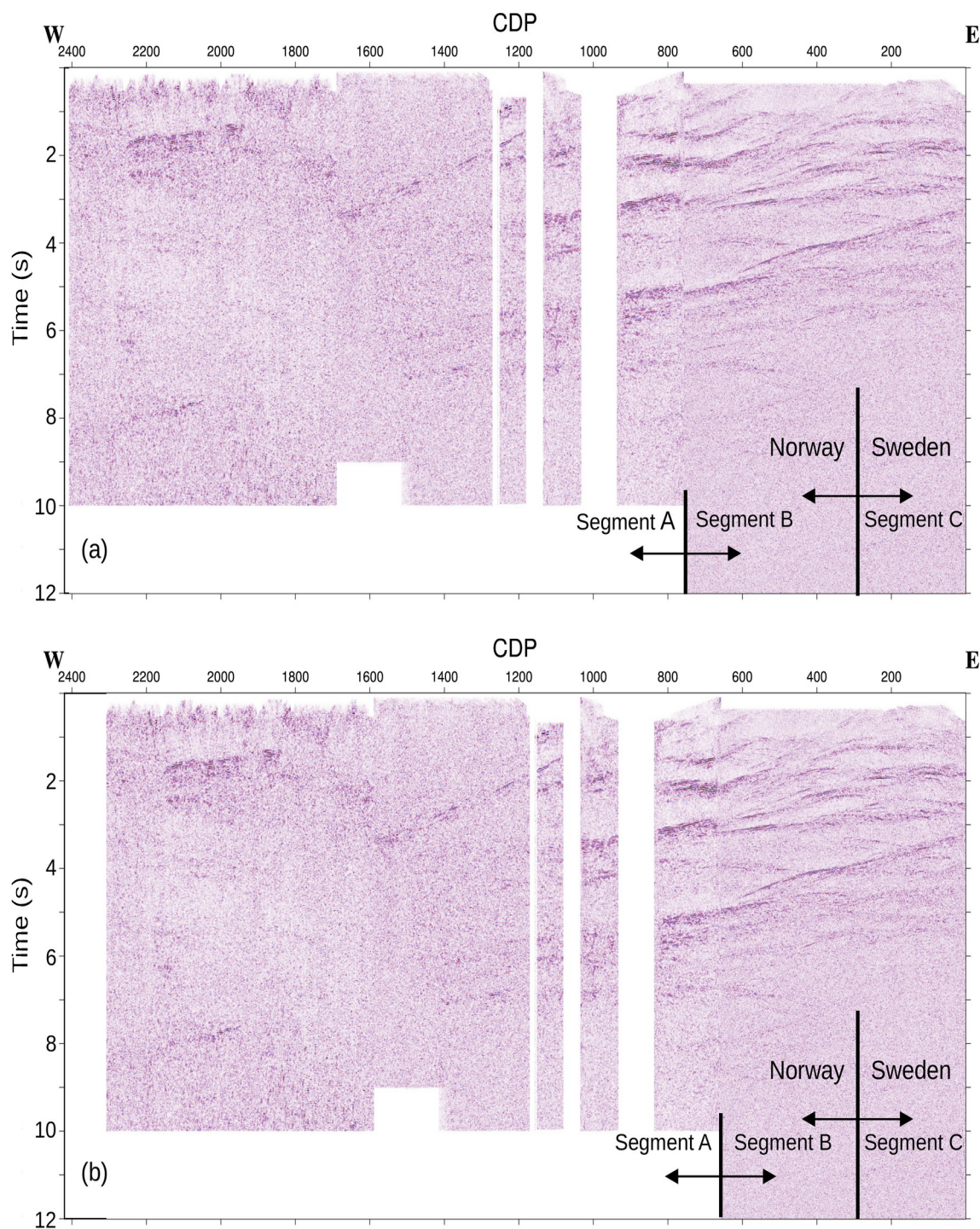
Figure 3: (a) Merged segments A, B and C as done by Lescoutre et al. (2022) and Roberts and Hurich (2018). (b) Merged segments
A, B and C in this paper. The new section now shows more continuity between segments A and B. Note that the CDP numbering
differs from that in Figures 1 and 2.
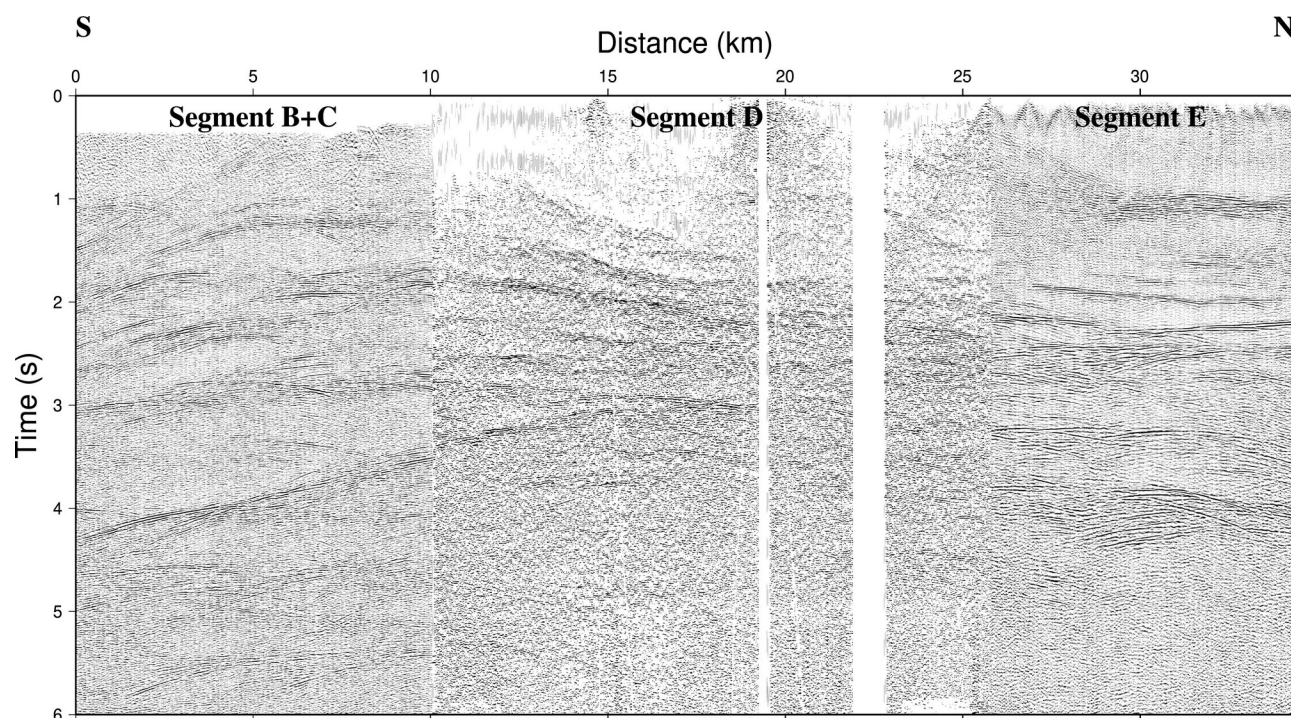
Figure 4: Merged segments C, D and E. Segment D was only available on paper and was digitized from the report in Palm et al. (1991). Figure shows that there is some 3D structure in the area and that is not clear what is the best way to merge segment C with segment E to generate a continuous W-E directed profile to migrate. Note also the clear diffracted energy on segments B, C and E.

130   As mentioned previously, the main differences between the present processing and previous versions are in the western part
of the merged profile. Figure 3a shows how Lescoutre et al. (2022) merged the Norwegian part of the CCT. This merging is
similar to that presented in Roberts and Hurich (2018), but does not take into account the overlap between segments A and B
(Figure 2). There is a clear break in the reflections where the two segments join. Based on Figure 2 there is about a 2.5 km
overlap between segments A and B. Given that the data signal to noise ratio on segment A (closer source spacing, higher

135   fold) is higher than segment B, we chose to retain the data from segment A and merge the two profiles about 2.5 km east of
the western end of segment B (Figure 3b). The reflections are now nearly continuous across the merger, allowing better
correlation between the two segments. Getting the merger point right becomes even more important for migration of the data
since abruptly ending reflections on stacked sections will generate "smiles" on the migrated sections.

The most problematic area for providing a continuous seismic profile is how to merge segments C and E since there is a

140   northward jump from the eastern end of C to the western end of E by about 15 km. Segment D connects these two profiles
and provides some guidance (Figure 4). The reflections in the upper 2.5 s have a clear northward dip component on the
western half of segment D and then flatten. The reflections between 2.5 s and 3 s are fairly horizontal and the distinct one
below 3 s has a southward dip on the western half, but then also becomes nearly horizontal towards the north. It is not
possible to project segment C onto segment E in a consistent manner so that all reflections become continuous across the

145   merger point. We choose to merge the two segments about 4 km east of the western end of segment E since this provides the

most continuous appearance (Figure 5), but with the flag that the upper 2.5 s should be treated with caution. Note the numerous diffractions both on the eastern end of segment C and the western end segment E (Figure 4), indicating significant faulting in this area. These diffractions do not appear on segment D, probably due to that the faults have a roughly N-S strike. Finally, we migrate the data shown in Figure 5 using Stolt migration and depth convert it with a 1D velocity function starting at 5500 m/s at the surface and increasing to a RMS velocity of 6000 m/s at 3 s (Figure 6).
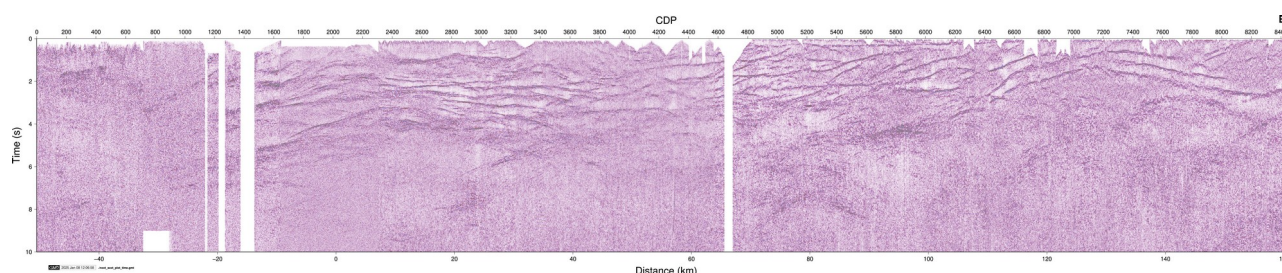
Figure 5: Segments A to C and E to J merged into a single stacked section as described in the text. CDP numbering corresponds to that shown in Figure 1.
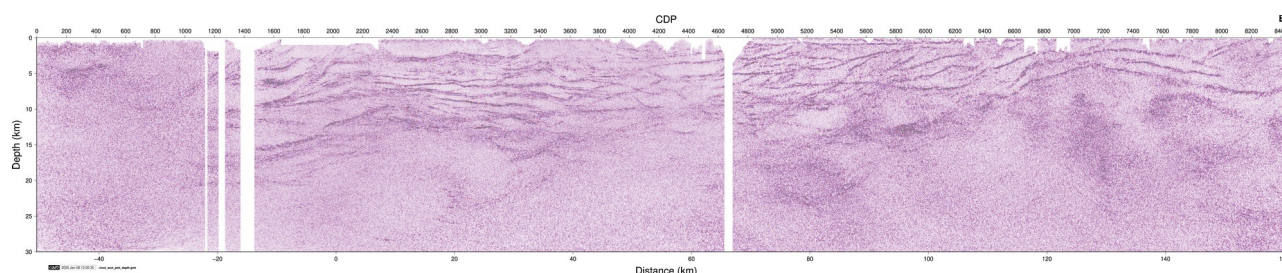
Figure 6: Stacked section in Figure 5 migrated and depth converted using a 1D velocity function starting at 5500 m/s at the surface and increasing to 6000 m/s at 3 s. CDP numbering corresponds to that shown in Figure 1.

5 Results and discussion

The depth converted image (Figure 6) obtained west of the border has some significant differences compared to that of Lescoutre et al. (2022) and Roberts and Hurich (2018). The main differences are due to migration in the CDP interval 1400 to 2200 where the diffractions have collapsed, revealing shorter reflective segments that appear offset to one another. Since most of these segments are either sub-horizontal or gently west dipping this appearance is not due to the merging process.

Our new geological interpretation (Figure 7) suggests that most of the flat-lying to moderately dipping reflections can be interpreted as representing dolerites within the Paleozoic basement, such as described in the central and western part of the profile (Lescoutre et al., 2022) and as observed in basement windows in the region (Johansson, 1980). Hauser (1990) suggested early on that much of the reflectivity could be due to the presence of dolerite sills. In detail, some of these reflections appear offset (top-to-the-east) along gently W-dipping reflections which, in contrast to the interpreted dolerites, appear as continuous (sometimes very discrete) reflections from the western part to the central part of the profile. Such

reflections are thus interpreted as due to contractional structures related to the Caledonian orogeny. We also observe some sub-horizontal reflections that show a normal offset across steep W-dipping horizons (sometimes inconspicuous).

In addition to the Kopperå fault as identified by Roberts and Hurich (2018) (marked by K in Figure 7), our results highlight

170 the Steinfjell normal fault (SF in Figure 7) bounding the Skardöra antiform to the east (Sjöström and Bergman, 1989). Along the Steinfjell fault, our reprocessing clearly images a thick deformation zone in its footwall with reflections showing downward drag or bending near the fault (grey lines on Figure 7). This fault seems to flatten at ~10 km depth. Below the Skardöra antiform (CDP 1900-2100), our results highlight a newly identified extensional fault zone which offsets the interpreted dolerites and supposedly the Caledonian thrust faults (e.g., at ~14 km depth). Its upward propagation is unclear as

175 shallow seismic reflections do not appear to be significantly offset.

In the hanging-wall of the Steinfjell fault, the strong reflections (interpreted as dolerites) show an upward dragging against the fault and highlight the downward displacement of the par-autochthonous basement west of the Skardöra antiform. Note that this interpretation significantly diminishes the thickness of the Upper Allochthon to the west of the Skardöra antiform (resulting in a shallower top basement depth) and reduces the extensional displacement along the Steinfjell fault to about 3 to

180 5 km. Our interpretation also implies that the Middle Allochthon unit is locally discontinuous or very thin in comparison to the interpretation by Hurich (1996).

To summarize, our reprocessing provides a clearer image of the bedrock architecture in the western part of the central Scandinavian Caledonides. It shows that the dolerite sill swarm propagates further west than generally previously interpreted and reveals new structural features that question the overall nappe stack geometry and the contractional/extensional

185 deformation in the par-autochthonous basement.
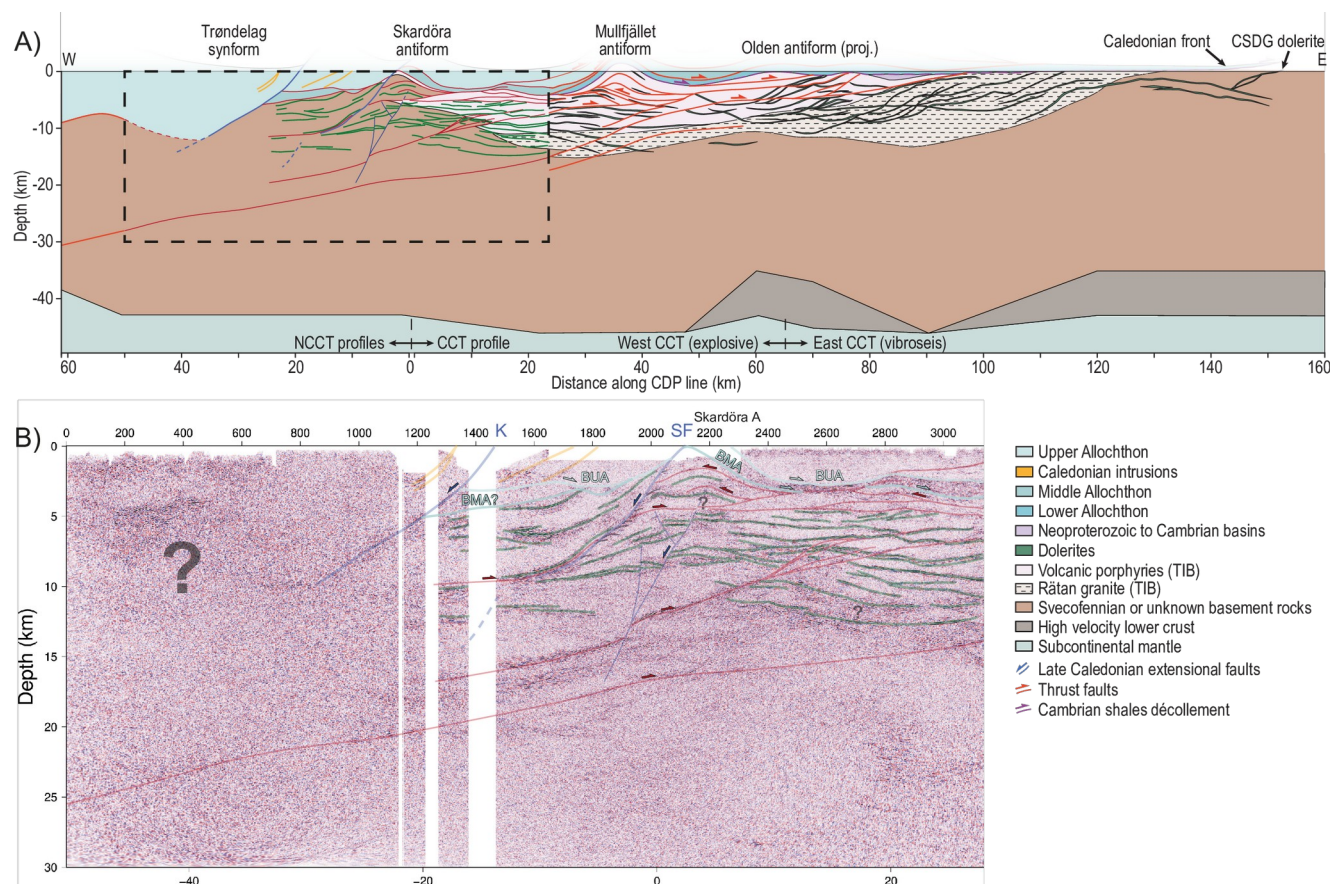
Fig 7: (A) Interpretation of the depth converted merged profile. The section eastwards of distance 25 km is the same as in Lescoutre et al. (2022) while the section west of this point is mainly new. (B) The seismic section below shows in more detail how the interpretation was made. D – Dolerite; BUA – Base Upper Allochthon; BMA – Base Middle Allochthon; K – Kopperå fault; SF – Steinfjell fault.

6 Conclusions

We present, for the first time, a complete migrated seismic section across the central Scandinavian Caledonides that includes available data both from the Norwegian side and the Swedish side. To produce the section different segments of the profile were resampled in space and time to a uniform interval. Gaps and overlap in the segments were carefully considered. Based on the depth converted migrated image a revised interpretation of the western part of the profile is made. In contrast to previous interpretations, we interpret the shorter sub-horizontal reflections in the Skärdöra antiform to originate from faulted dolerite sills rather than shear zones. Results from the COSC-2 drilling further east support this interpretation where reflections of similar character are also present. It is likely that the dolerite system encountered there continues west into the Skärdöra antiform. If correct, then our interpretation implies that the Upper Allochthon to the west of the Skärdöra antiform is significantly thinner than suggested in previous studies and that the extensional displacement along the Steinfjell fault is

200 about 3 to 5 km, less than previously inferred. Furthermore, the Middle Allochthon may be locally discontinuous or very thin west of the Skärdöra antiform.

Data availability

To request the data associated with this research, contact the corresponding author of the article after the publication of this work.

Author contribution

205 CJ and RL conceptualized and designed this study. CJ was responsible for the data processing. RL, BA and CJ led the geological interpretation. CJ wrote the initial draft with input from RL and BA. All authors contributed to the results and discussion and approved the submission of this paper.

Competing interests

210 The authors acknowledge that there are no conflicts of interest.

Acknowledgments

We thank Norwegian and Swedish Research Councils for their support in the 1980s and 1990s towards this work. We thank Chuck Hurich for making the seismic sections on the Norwegian side available for our use.

Supplementary material

215 Higher resolution versions of Figures 5 and 6 are presented in the supplementary material.

References

Almqvist, B.S.G., van der Lelij, R., Högdahl, K., Lescoutre, R., Schönenberger, J., Fossen, H., Sjöström, H., Juhlin, C., Luth, S., Grigull, S. And Viola, G.: Brittle basement deformation during the Caledonian Orogeny observed by K-Ar geochronology of illite-bearing fault gouge in west-central Sweden. Terra Nova, doi:10.1111/ter.12645, 2023.
220

Andersson, J., Claesson, S. and Kooijman, E.: Age and crustal affinity of Precambrian basement nappes and underlying basement in the east central Scandinavian Caledonides. Geological Society of Sweden 150-year anniversary meeting, extended abstract, 2022.

225 Arnbom, J.-O.: Metamorphism of the Seve Nappes at Åreskutan, Swedish Caledonides. Geologiska Föreningen för Stockholm Förhandlingar, 102, 359-371, doi:10.1080/11035898009454493, 1980.

Gee, D.G., and Stephens, M.B.: Regional context and tectonostratigraphic framework of the early-middle Paleozoic Caledonide orogen, northwestern Sweden. Geological Society, London, Memoirs, 50, 481-494, doi:10.1144/M50-2017-21, 2020.

230

Hauser, E.C.: Comment and Reply on Deformation of the Baltic continental crust during Caledonide intracontinental subduction: views from seismic reflection data, Geology, 18, 578-580, doi:10.1130/0091-7613(1990)018%3C0578:CARODO%3E2.3.CO;2, 1990.

235 Hurich, C. A.,; Kinematic evolution of the lower plate during intracontinental subduction: An example from the Scandinavian Caledonides. Tectonics, 15, 1248–1263, doi:10.1029/96TC00828, 1996.

Hurich, C. A., Palm, H., Dyrelius, D., and Kristoffersen, Y.: Deformation of the Baltic continental crust during Caledonide intracontinental subduction: Views from seismic reflection data, Geology, 17, 423–425, doi:10.1130/0091-7613(1989)017%3C0423:DOTBCC%3E2.3.CO;2, 1989.

240

Jakob, J., Andersen, T.B., Mohn, G., Kjøll, H.J. and Beyssac, O.: Revised tectono-stratigraphic scheme for the Scandinavian Caledonides and its implications for our understanding of the Scandian orogeny. The Geological Society of America Special Paper 554, 335-374, doi:10.1130/2022.2554, 2022.

245

Jeanneret, P., Klonowska, I., Barnes, C., Majka, J., Holmberg, J., Gilio, M., Nachlas, W., Alvaro, M., Kośmińska, K., Lorenz, H., Zack, T., Ladenberger, A. and Koyi, H.: Deciphering the tectonometamorphic history of subducted metapelites using quartz-in-garnet and Ti-in-quartz (QuiG-TiQ) geothermobarmometry – A key for understanding burial in the Scandinavian Caledonides. Journal of Metamorphic Geology, doi:10.1111/jmg.12693, 2023.

250

Johansson, L.: Petrochemistry and regional tectonic significance of metabasites in basement windows of the central Scandinavian Caledonides, Geologiska Föreningen i Stockholm Förhandlingar, 102(4), 499–514. doi:10.1080/11035898009454503, 1980.

255   Juhojuntti, N., Juhlin, C., and Dyrelius, D.: Crustal reflectivity underneath the Central Scandinavian Caledonides, Tectonophysics, 334, 191–210, doi:10.1016/S0040-1951(00)00292-4, 2001.

Klonowska, I., Janák, M., Majka, J., Petrík, I., Froitzheim, N., Gee, D.G. and Sasinkova, V.: Microdiamond on Åreskutan confirms regional UHP metamoprhism in the Seve Nappe Complex of the Scandinavian Caledonides. Journal of
260   Metamorphic Geology, 35, 541-564, doi:10.1111/jmg.12244, 2017.

Lehnert, O., Almqvist, B., Anderson, M., Andersson, J., Cuthbert, S., Calner, M., Carter, I., Callegari, R., Juhlin, C., Lorenz, H., Madonna, C., Meinhold, G., Menegon, L., Klonowska, I., Pascal, C., Rast, M., Roberts, N.M.W., Ruh, J.B. and Ziemniak, G.: The COSC-2 drill core and its well-preserved lower Palaeozoic sedimentary succession – an unexpected treasure beneath the Caledonian nappes. Estonian Journal of Earth Sciences, 73, 2, 134-140, doi:10.3176/earth.2024.13.,
265   2024.

Lescoutre, R., Almqvist, B., Koyi, H., Berthet, T., Hedin, P., Galland, O., Brahimi, S., Lorenz, H. and Juhlin, C.: Large-scale, flat-lying mafic intrusions in the Baltican crust and their influence on basement deformation during the Caledonian orogeny, GSA Bulletin, 134, 3022–3048, doi:10.1130/B36202.1, 2022.

270

Lescoutre, R., Söderlund, U., Andersson, J. and Almqvist, B.: 1.47 Ga and 1.27–1.26 Ga dolerite sheets within the basement underneath the east-central Scandinavian Caledonides. Geological Society of Sweden 150-year anniversary meeting, extended abstract, 2022.

275   Lorenz, H., Rosberg, J.-E., Juhlin, C., Klonowska, I., Lescoutre, R., Westmeijer, G., Almqvist, B.S.G., Anderson, M., Bertilsson, S., Dopson, M., Kallmeyer, J., Kück, J., Lehnert, O., Menegon, L., Pascal, C., Rejkjær, S. and Roberts, N.: COSC-2 – drilling the basal décollement and underlying margin of paleocontinent Baltica in the Paleozoic Caledonide Orogen of Scandinavia, 30, 43-57, doi:10.5194/sd-30-43-2022, 2022.

280   Majka, J., Rosén, Å., Janák, M., Froitzheim, N., Klonowska, I., Manecki, M., Sasinkova, V. and Yoshida, K.: Microdiamond discovered in the Seve Nappe (Scandinavian Caledonides) and its exhumation by the "vacuum-cleaner" mechanism. Geology, 42, 1107-1110, doi:10.1130/G36108.1, 2014.

Palm, H., Gee, D., Dyrelius, D., and Björklund, L.: A reflection seismic image of Caledonian structure in central Sweden:
285   Sveriges geologiska undersökning, Serie Ca. Avhandlingar och uppsatser NR 75, 1991.

Roberts, D. and Hurich, C.: The concealed Kopperå fault: A half-graben bounding structure located along the eastern flank of the Trøndelag depression, mid-Norway, Norges geologiske undersøkelse Bulletin, 456, 1-10., 2018.

290 Robinson, P., and Roberts, D.: A tectonostratigraphic transect across the central Scandinavian Caledonides, Storlien – Trondheim – Lepsøy Part II. Excursion guide in Norway. NGU Report 2008.064, 2008.

Saalmann, K., Bjerkgård, T., Slagstad, T., Sandstad, J.S., Lutro, O., Keiding, J., Snook, B. and Angvik, T.L.: Revised tectonostratigraphy and structural evolution of the Köli Nappe Complex, Central Caledonides in Nordland, Norway, 178, doi:10.1144/jgs2020-214, 2021.

295

Sjöström, H., and Bergman, S.: Asymmetric extension and Devonian(?) normal faulting; examples from the Caledonides of eastern Trøndelag and western Jämtland, Geologiska Föreningen i Stockholm Förhandlingar, 111(4), 407–410. doi:10.1080/11035898909453148, 1989.

300 Sopher, D.: Converting scanned images of seismic reflection data into SEG-Y format, Earth Sci. Inform., 11, 241–255. doi:10.1007/s12145-017-0329-z, 2018.

Söderlund, U., Elming, S.-Å., Ernst, R.E. and Schissel, D.: The central Scandinavian dolerite group – Protracted hotspot activity or back-arc magmatism?: Constraints from U-Pb baddeleyite geochronology and Hf isotopic data, Precambrian
305 Research, 150, 136-152, doi:10.1016/j.precamres.2006.07.004, 2006.

Törnebohm, A.E.: Om fjällproblemet. GFF, 10, 328–336, doi:10.1080/11035898809444211, 1888.